# Circuit Techniques for Wireless Bioelectrical Interfaces

*(Invited Paper)*

M. Nagaraju, J. Silver, F. Zhang, Y. Liao, J. Pandey, T. Morrison, A. Mishra, D. Yeager, B. Otis

Department of Electrical Engineering, University of Washington, Seattle, WA, 98195, USA

***Abstract***— Recent advances in integrated circuit technology scaling, analog circuitry, and wireless communication have created the possibility for complex low noise, low power wireless instrumentation to be deployed in previously impossible scenarios, particularly in the realm of wireless sensing for biology research and biomedical applications. The generation of portable, autonomous devices made possible by these improvements will allow, for example, unobtrusive long-term health monitoring by way of fully implantable clinical diagnostic systems. This paper presents some achievements made to this end, and describes the circuit design techniques and system architectures used to realize low power wireless bioelectrical interfaces.

## I. Introduction

State-of-the-art advances made in the realm of wireless circuit technology are opening the door to a new breed of body-worn devices. For example, portable neuroprostheses promise to improve the quality-of-life for people with mobility disorders. Wireless EMG technology could enable remote therapy and advanced human-computer interfaces. Miniaturized low power wireless technology will allow previously impossible freely-behaving animal research. Such systems will require closed loop recording, analysis, and stimulation performed under a strict power budget. Size and power reduction necessitated in the rapidly evolving area of biosignal monitoring are placing increasingly stringent demands on integrated circuit technology and circuit designers. This paper discusses the technology behind and applications of low power, wireless communication circuitry for bioelectrical interfaces.

The rest of the paper is organized into five sections. Section II discusses the motivation for and system requirements of a new generation of wireless biosignal interface systems. Sections III and IV present two contrasting paradigms for the realization of such systems, active vs. passive. Section III introduces an active (battery-powered) implementation of a wireless neural interface, the 'Bumblebee' while Section IV reviews several passive (battery-free) realizations. An initial realization of a wirelessly-powered, functional contact lens is presented in Section V, and concluding remarks are given in Section VI.

## II. Applications and System Requirements of Autonomous Bioelectrical Interfaces

The deployment of electrical interfaces for biological research and medical applications places strict requirements on system power and biocompatibility. For long-term health monitoring applications, the risk of infection may be prohibitively high to allow wires or connectors to penetrate the skin. Hence, in addition to low-power recording, biosignal interfaces should provide methods of wirelessly transmitting acquired signals to an external monitoring device. Robust, multichannel wireless devices for neural signal acquisition are a critical development that will permit brain-computer interfaces (BCI) and neuroprostheses to gain widespread acceptance for the study and treatment of neurological disorders. The additional burden of transmission increases the constraint on the power budget. In addition, chronic recording of bioelectrical signals in humans, or recording in very small animals and insects, necessitate a small form-factor for the wireless, miniaturized biosignal interface. These requirements lead to two, somewhat competing, paradigms in bioelectrical interfaces, namely active and passive systems. An active system employs an on-board battery and enables long-term monitoring and far-field transmission. However, the inclusion of a battery necessitates frequent replacement which may be prohibitive, particularly in human BCI implementations. In contrast, the passive interface derives its energy from an energy harvester such as a Thermoelectric Generator (TEG) and may employ a low-power boost converter or RF-to-DC rectifier to power the active circuitry [1], [2]. In the following sections, we discuss prototype systems, both active and passive, successfully implemented for in-vivo data acquisition and wireless transmission.

The information in the brain could be recorded as electrical signals generated by individual neurons in the form of action potentials, or spikes. As the recording site is moved away from a single neuron, it captures electrical activity from multiple sources. Any interface circuit should be able to acquire the signal in the frequency band of interest while rejecting the large DC offset resulting from the electrode tissue interface.

Spike recordings generally have high frequency content and a wide range of signal amplitudes approximately between 20$\mu$V and 500$\mu$V. Most of the neural activity lies within the range of 0.1-10kHz. Local field potentials (LFP) reflect the summed activity of an ensemble of neurons and are hence indirect measures of neural processing. LFP measurements are less susceptible to chronic measurements and avoids the problem of tissue encapsulation and micromotion encountered in single-unit recordings [3]. Frequency bands of interest in the LFP include the Alpha

978-1-4244-5271-2/10/$26.00 ©2010 IEEE 

(5-10Hz), Beta (15-30Hz) and high Gamma (80-200Hz). Typical amplitudes of field potentials measure 5-300$\mu$V.

## III. Bumblebee - A 560$\mu$W active neural Tag

In this section, we describe the 'Bumblebee', a wireless biosignal interface with a battery on board capable of transmitting neural data over a range of 10m. The form factor of the system is 0.1cm$^3$ and it weighs 0.3gm (Fig. 1). This enables the observation of brain activity in small animals such as mice and moths. The system consumes 560$\mu$W when powered by a Zinc Air Size 5 battery.

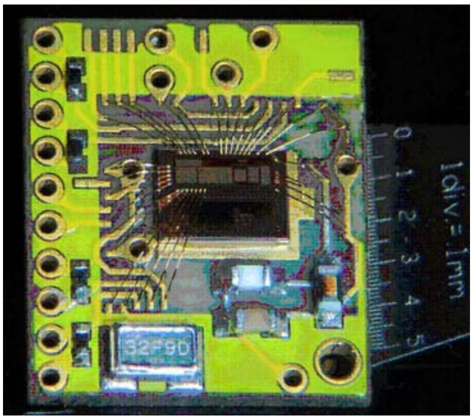


Fig. 1. Neural Recording and Tranmission Chip.

The system is based on the 2$^{\text{nd}}$generation of the wireless neural interface chip presented in [4]. The architecture of the system is shown in the Fig. 2. It consists of an analog front-end providing a gain of 40-78dB over a 25mHz to 11.5kHz bandwidth. The LNA inputs are AC-coupled using 20pF capacitors and high-resistance($> 100\text{G}\Omega$) MOS-bipolar pseudo-resistors [5]. Additionally, the input signal drives both the NMOS and PMOS transistors to effectively double the transconductance for the same bias current [6] and thus achieves the best reported Noise Efficieny Factor (NEF) to date for fully differential amplifiers. To accomodate varying amplitudes of the spike recordings, a VGA with a gain range of 2-38dB is used. The output of the front-end is sampled by an 8-bit successive approximation (SAR) ADC which reduces power consumption [7]. The ADC is designed to operate at sample rates from 10-100 kSps.

Traditional transmitters utilizing a power amplifier (PA) are not suitable for low-power applications and hence we propose a frequency-multiplying scheme with an edge-combiner driving a matched load acting as the PA. The baseband FSK data modulates the capacitive pulling on the crystal to create a frequency shift of 16.4kHz which is multiplied by 9$\times$ to create FSK data in the MICS band. We use a low-power Delay-locked loop (DLL) for frequency multiplication. To prevent unequal delays from the delay

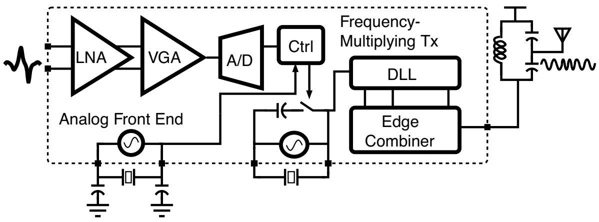


Fig. 2. Architecture of the active wireless neural recording and transmission system.

cells which result in frequency spurs at the output, we employ a dual-edge locking scheme.

The Bumblebee system has been configured for recording and transmission of EMG signals. A commercial off-the-shelf USB reciever was used to demodulate the transmitted data. Fig. 3 shows the reconstructed EMG signal from three arm movements at a distance of 10m. Due to its ultra-low-power consumption, the system can operate continuously for approximately 70 hours with a Zinc Air size 5 battery.

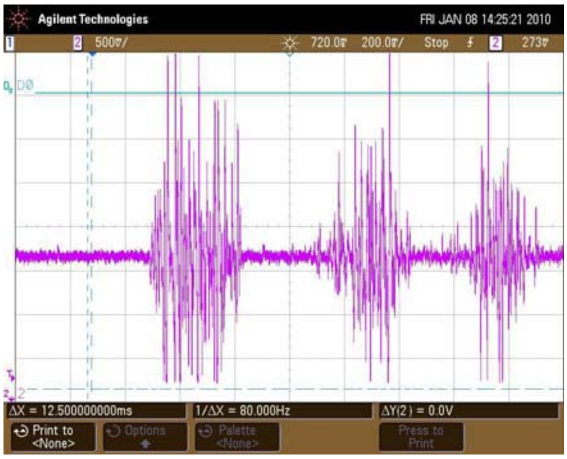


Fig. 3. Reconstructed EMG signal from a USB reciever at a distance of 10m.

## IV. RFID Tag based wireless bioelectrical interfaces

A passive neural interface harvesting power from RF energy provided by a commercial UHF RFID reader eliminates the need for a battery on board. This would enable continuous monitoring of neural signals reducing the need for replacement surgeries and neural recording from small animals and insects which is impossible with an active system. RFID technology allows the energy harvester to be placed at distance of greater than 1m, opening the possibility of indefinite operation without the need for battery replacements. In this section, we outline the implementation of two RFID-based wireless interfaces.

## A. Neural WISP

A new platform called Neural WISP (Wireless Identification and Sensing Platform) which harvests power from a commercial UHF RFID reader is implemented [8]. A system diagram of the Neural WISP is shown in the Fig. 4. It utilizes an ultra-low-power, programmable microcontroller in an interrupt-driven mode to reduce power consumption. The microlevel neural signals are first amplified and then fed to a spike detector to reduce the data rate. An input spike wakes up the microcontroller ($\mu$C), which increments the spike count and enters sleep mode again. A timing driven interrupt signals the end of the counting mode and wakes up the $\mu$C for communication with the reader.

A commercial UHF RFID reader powers the WISP, and communicates via the EPC Class 1, Gen 2 protocol. An on-board RF rectifier, voltage booster and storage capacitor enables full passive operation of the WISP. The use of a programmable $\mu$C allows WISP to be easily configured for different applications, including measurement of temperature, light level, strain, and acceleration.

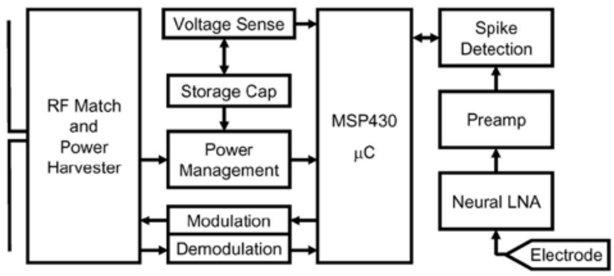


Fig. 4. System diagram of the Neural WISP

The Neural WISP was used in the *in-vivo* measurements on a macaque monkey and Fig. 5 shows the recorded spikes after digitizing and high-pass filtering offline.

## B. Passive RFID Tag

A fully-integrated single-chip 900MHz RFID-based sensing tag suitable for neural recording in small animals is implemented [9]. The sensing tag includes a 1.25$\mu$Vrms integrated noise chopper-stabilized micropower amplifier, and an 8b ADC in the analog front-end (Fig. 6). Chopper-stabilizion provides extremely low-input referred noise for low frequency amplifiers by upmodulating and filtering the flicker noise [10]. The neural tag generates a unique tag ID based on process variation, eliminating the need of an SRAM [11]. It employs an on-chip RF rectifier with a 6-stage charge pump and is powered and read from a commercial RFID reader with a 6dBi patch antenna. The chip contains a 1.2V bandgap reference and three sub-microwatt regulators to power the various blocks.

The entire system weighs 0.25g, measures less than 1cm$^2$ and is suitable for neural sensing in insects and small

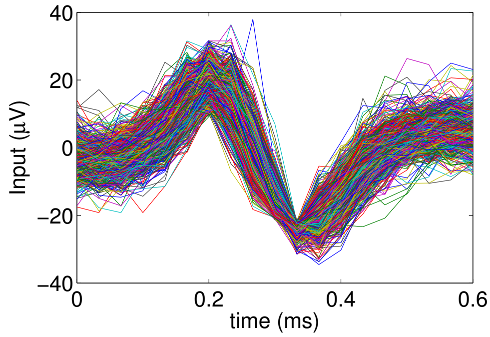


Fig. 5. Neural spikes collected from a monkey through Neural-WISP's analog front end.

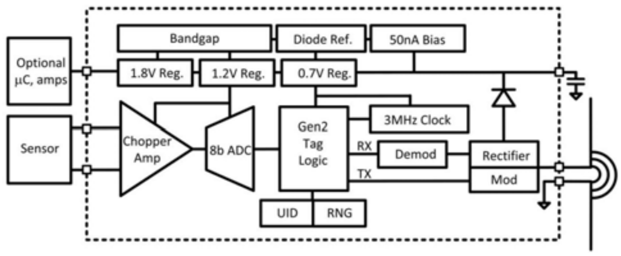


Fig. 6. System Architecture of the SOC RFID tag

animals. It was mounted on a Manduca Sexta (Hawkmoth) to record the in-flight core body temperature using a 36AWG Type-T (copper-constantan) thermocouple. This moth species generates a substantial temperature increase from ambient temperature before flight. We were able to perform a wireless, battery-free experiment using our passive neural tag. Fig. 7 shows the *in-vivo* data recorded during the flight plotted versus time. The entire system inclusive of the thermocouple weighs 0.35g and enables long-term recording.

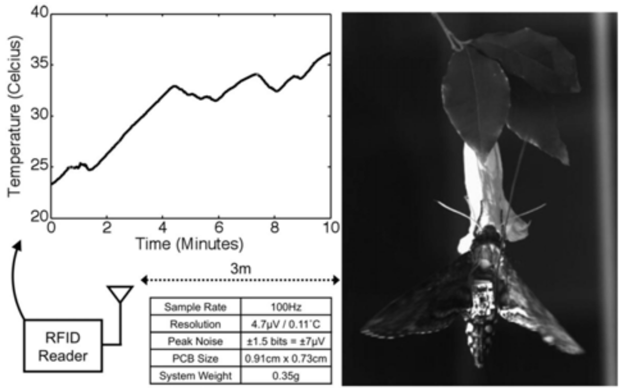


Fig. 7. *In-vivo* data and deployment graph

## V. RF Powered Active Contact Lens

As a final example, we explore integrating circuitry onto a contact lens. Useful biomarkers exist in the blood such as the glucose level, which potentially be sensed through a contact lens on the surface of the eye. Advances in electronics and photonics have enabled the integration of sensing and display devices on a contact lens. This requires the design of ultra low-power miniaturized energy harvesting circuit, biosensor, display circuitry and a transceiver. To prototype such a system, we present an active contact lens with an RF power harvester, power management circuitry and a micro-led for display (Fig. 8). The system has a custom-designed gallium aresenide LED which is duty-cycled to 3% at 1MHz to reduce the power requirement. A loop antenna was chosen to facilitate integration on the lens. The RF power harvesting circuits, power management system and storage capacitor was fabricated in a $0.13\mu$m process. An eight-stage rectifier design was chosen for maximum efficiency, output voltage and matching of the input impedance. The difficulty in realizing high quality tank circuits on the plastic susbtrate and extemely small size of the chip prevents any passive impedance matching tank circuit resulting in loss of sensitivity of the rectifier.

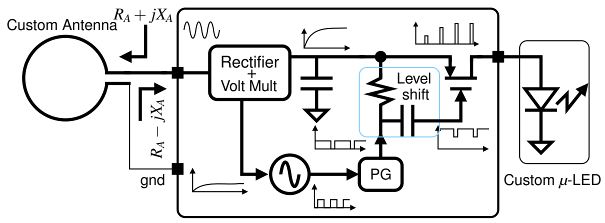


Fig. 8. Architecture of the custom chip on Contact lens

Fig. 9 shows the waveform controlling the LED turn-on. We use a 2GHz dipole antenna at the RF reader and are able to achieve an LED turn-on range of 2mm using a 25dBm RF source. Thus, we are operating well within the near field of the dipole antenna. The poor range of operation can be attributed to antenna efficiency, suboptimal matching, and low dipole antenna directivity. With a modified antenna fabrication process, transmit antenna, and improved matching, we expect far field operation.

## VI. Conclusion

The ongoing development of autonomous biointerface circuits and systems is crucial for the advancement of bioscience research and human health monitoring. Performance requirements for these systems and design techniques employed to meet them have been presented. Measured performance results have been given, along with *in-vivo* test data acquired with several of these systems.

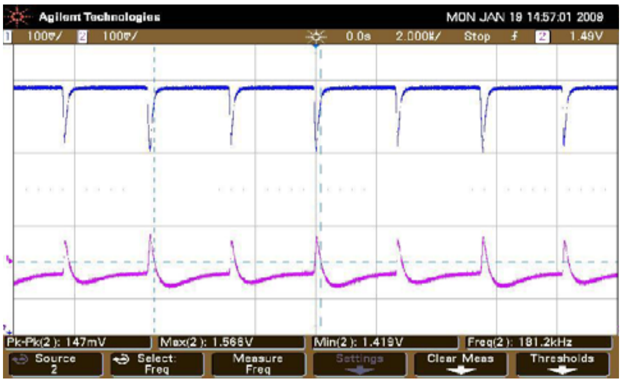


Fig. 9. The level-shifted duty-cycled pulse and the voltage pulses applied to the $\mu$-LED

## Acknowledgment

The authors would like to acknowledge the assistance provided by Prof. Chet Moritz, Prof. Steve Perlmutter and Prof. Eberhard Fetz in *in-vivo* recordings.

## References

[1] E. Carlson, K. Strunz, and B. Otis, “20mv input boost converter for thermoelectric energy harvesting,” in *VLSI Circuits, 2009 Symposium on*, June 2009.

[2] D. Yeager, A. Sample, and J. Smith, “WISP; A Passively Powered UHF RFID Tag with Sensing and Computation,” *RFID Handbook: Applications, Technology, Security, and Privacy*, 2008.

[3] D. Heldman, W. Wang, S. Chan, and D. Moran, “Local field potential spectral tuning in motor cortex during reaching,” *Neural Systems and Rehabilitation Engineering, IEEE Transactions on*, vol. 14, no. 2, pp. 180 –183, June 2006.

[4] S. Rai, J. Holleman, J. Pandey, F. Zhang, and B. Otis, “A 500$\mu$W Neural Tag with 2$\mu$Vrms AFE and Frequency-Multiplying MICS/ISM FSK Transmitter,” *IEEE ISSCC Dig. Tech. Papers*, Feb. 2009.

[5] R. Harrison and C. Charles, “A low-power low-noise cmos amplifier for neural recording applications,” *Solid-State Circuits, IEEE Journal of*, vol. 38, no. 6, pp. 958 – 965, June 2003.

[6] J. Holleman and B. Otis, “A sub-microwatt low-noise amplifier for neural recording,” in *Proc. IEEE Engineering in Medicine and Biology Society Conference*, August 2007, pp. 3930–3933.

[7] J. Holleman, A. Mishra, C. Diorio, and B. Otis, “A spike detector and feature extractor in .13$\mu$m cmos,” *Custom Integrated Circuits Conference, 2008. CICC’08. IEEE*, 2008.

[8] D. Yeager, J. Holleman, R. Prasad, J. Smith, and B. Otis, “Neuralwisp: A wirelessly powered neural interface with 1-m range,” *Biomedical Circuits and Systems, IEEE Transactions on*, vol. 3, no. 6, pp. 379 –387, Dec. 2009.

[9] D. Yeager, F. Zhang, A. Zarrasvand, and B. Otis, “A 9.2$\mu$A Gen 2 Compatible UHF RFID Sensing Tag with -12dBm Sensitivity and 1.25$\mu$Vrms Input-Referred Noise Floor,” *IEEE ISSCC Dig. Tech. Papers*, Feb. 2010.

[10] T. Denison, K. Consoer, W. Santa, A.-T. Avestruz, J. Cooley, and A. Kelly, “A 2$\mu$w 100 nv/rthz chopper-stabilized instrumentation amplifier for chronic measurement of neural field potentials,” *Solid-State Circuits, IEEE Journal of*, vol. 42, no. 12, pp. 2934 –2945, Dec. 2007.

[11] Y. Su, J. Holleman, and B. Otis, “A digital 1.6 pj/bit chip identification circuit using process variations,” *Solid-State Circuits, IEEE Journal of*, vol. 43, no. 1, pp. 69 –77, Jan. 2008.